STACKED INSULATOR INDUCTION ACCELERATOR GAPS

T.L. Houck, G.A. Westenskow, Lawrence Livermore National Laboratory, Livermore, CA 94551
J.-S. Kim, S. Eylon, E. Henestroza, Fusion and Accelerator Research, San Diego, CA 92122
S.S. Yu, D. Vanecek, Lawrence Berkeley National Laboratory, Berkeley, CA 94720

Abstract

Stacked insulators, with alternating layers of insulating material and conducting film, have been shown to support high surface electrical field stresses. We have investigated the application of the stacked insulator technology to the design of induction accelerator modules for the Relativistic-Klystron Two-Beam Accelerator program. The rf properties of the accelerating gaps using stacked insulators, particularly the impedance at frequencies above the beam pipe cutoff frequency, are investigated. Low impedance is critical for Relativistic-Klystron Two-Beam Accelerator applications where a high current, bunched beam is transported through many accelerating gaps. An induction accelerator module designs using a stacked insulator is presented.

1 INTRODUCTION

Induction accelerators are a unique source for high-current, high-brightness, charged particle beams. Induction accelerators are used to drive very high-power microwave sources such as free electron lasers and relativistic klystrons, as intense-xray sources for radiographic applications, and as intense beam sources for material processing. Induction accelerators also are expensive, and the higher energy induction accelerators have been limited to major national laboratories. For these accelerators to become commercially viable, the basic unit of the accelerator, the induction module, must be made more compact, efficient, and less costly.

Novel accelerating gap designs for induction modules based on developing insulator technology provide an opportunity to move induction accelerators from expensive research devices into commercial applications. These novel high-gradient insulators (HGI's), comprised of finely spaced, alternating layers of dielectric and metal, have demonstrated much greater (factors of 1.5 to 4 times) vacuum surface flashover capability than insulators made from a uniform dielectric [1,2]. The HGIs also maintained similar capability in the presence of a cathode and electron beam [3]. The high field stress level in the presence of a beam can permit greatly simplify designs for accelerating gap. In typical induction accelerator designs [4], the gap is shaped to accommodate an extended insulator that is hidden from line-of-sight view of the beam. The shape of the gap must be carefully designed to minimize field stress on the vacuum surfaces.

The rf characteristics of the gap are an important consideration. The transverse interaction impedance of the gap with the beam can lead to collective beam instabilities. The longitudinal impedance can also be an important parameter in some applications, e.g. RK-TBA's. Recent measurements [5,6] of simplified gaps including stacked insulators have shown that the HGI's can improve the rf characteristics over that of a solid insulator.

Figure 1. Schematic of an accelerator induction module using a high-gradient insulator.

2 ACCELERATOR MODULE DESIGN

We have designed an induction module suitable for use in the proposed TBNLC relativistic klystron [7]. The performance specifications for the TBNLC induction module are comprehensive and demanding, and, prior to our design, no design had met all the specifications. An illustration of our module design is shown in Figure 1. The design must also be consistent with the beam focusing scheme that uses periodic quadrupole magnets.

2.1 RF Characteristics

The transverse impedance for a cavity can be estimated from $Z_\perp = 120\,\eta\ w/b^2$ ohms/m [8], where w is the gap width and b is the beam pipe radius. η is a design quality factor of order unity and determined by the de-Q-ing of the cavity. In our design, w = 1 cm and b = 2.3 cm. The desired $Z_\perp$ is $\leq 5,400$ Ω/m. This leads to a modest value of 2.3 for η (most designs have $1.3 < \eta < 1.9$). The desired longitudinal impedance, Z_L, is less than 2.5 Ω at 11.4 GHz, a difficult value to achieve. Changing η to reduce $Z_\perp$ tends to increase the minimum value of Z_L.

The transverse impedance was initially studied with URMEL to determine the field structure of the trapped dipole modes. This information was used to determine appropriate locations for placement of absorbing (de-Q-ing) material within the cell. An induction module design code, AMOS, was then used to calculate the impedances of the module with ferrite absorbers. Results of AMOS calculations are shown in Fig. 2 and 3. $Z_\perp$ decreases to a negligible level above 7 GHz. Z_L is shown over the range of interest. The power spectrum of the modulated current is only significant at 11.424 GHz ± 10 MHz.

2.2 Transverse Beam Dynamics

Transverse beam dynamics were examined with the MBBU code [9] using AMOS generated wakefields. The wakefield associated with the impedance in Fig. 2 is shown in Fig. 4. Shown are the transverse wakefields of a 11.4 GHz gaussian bunch with standard deviation length of 1.875 mm for the distribution. For clarity, wakefields up to about 114 bunch spacings are shown. The open circles indicate the wakefields at bunch centers. Higher
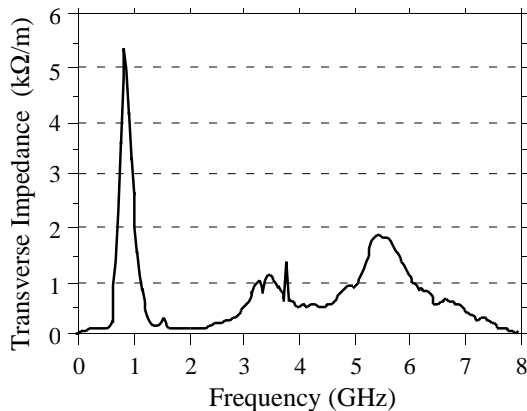
Figure 2. Transverse impedance spectrum.
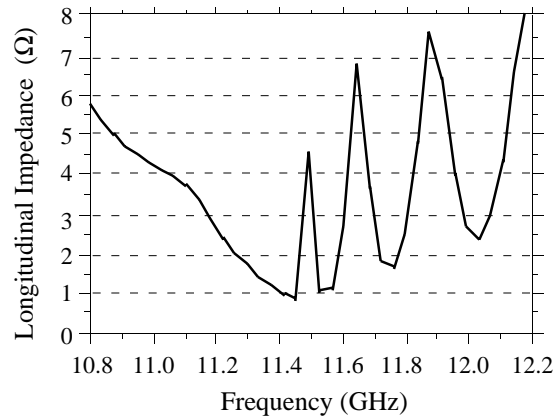
Figure 3. Longitudinal impedance spectrum.

wakefields are seen for the shorter bunches. Since BBU is cumulative over many bunches and structures, a small increase in wakefield magnitude results in a large growth in transverse motion. The effect of bunch length needs to be considered with respect to BBU growth.

In Fig. 5, we summarize the BBU growth for 1,000 bunches using the MBBU code for the wakefield of the Gaussian bunch (solid line in Fig. 4). The initial beam displacements were assumed to be uniform with no transverse momentum. An average beam current of 600 A with energy of 10 MeV, and betatron length of 2 m are considered.
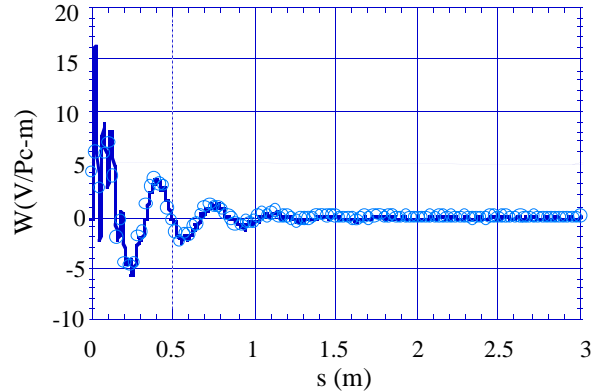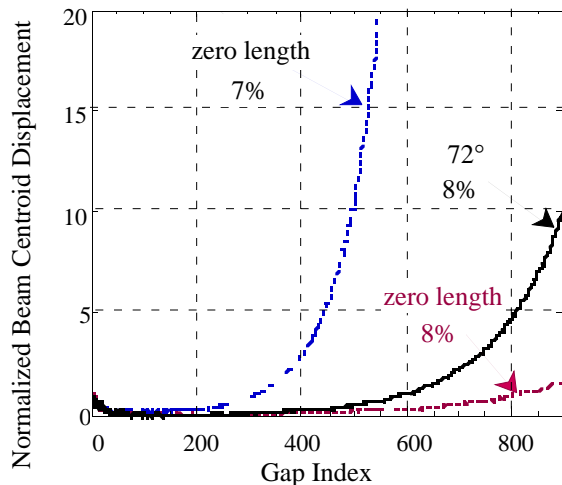

Figure 4. Dipole wakefield for impedance in Fig. 2.

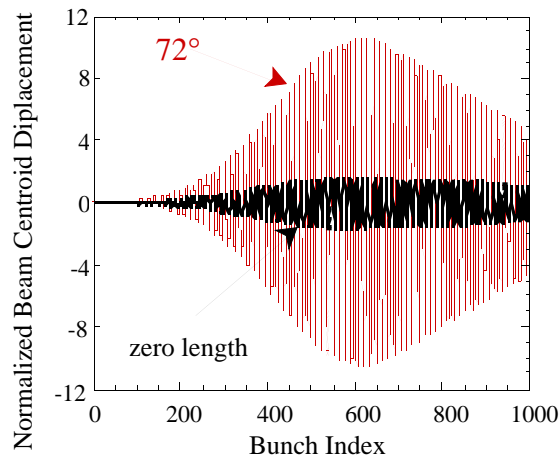Figure 5. BBU growth for different energy spreads and different bunch lengths.

Figure 6. Beam centroid displacements at 900th gap exit.

The dotted lines in Fig. 5 summarizes the BBU growth for various energy spreads. For energy spreads of $\geq \pm 8\%$, the BBU is reduced to an acceptable level over 900 structures by Landau damping. The solid line in Fig. 5 includes the wakefield effect within a bunch; each bunch is uniformly divided into 3 slices over 72° of a bunch wavelength. Each slice is represented by 30 microparticles for all cases. Fig. 6 shows normalized beam centroid displacements at the exit of the 900th gap.

2.3 Electric Field Stresses

Poisson was used to determine electrical field stresses in the gap. An equipotential plot for the gap design is shown in Fig. 7. The highest vacuum electrode fields are 120 kV/cm along the entrance to the gap and are acceptable for 300 ns pulses [10]. The electric field across the stacked insulator is a uniform 100 kV/cm. We expect that the stacked insulator will support nearly 200 kV/cm without breakdown. The method of assembling the gap in the cell readily allows for special treatment, e.g. electropolishing, of the high field stress surfaces if a greater safety margin is desired. On the oil side of the gap, the highest surface electric field is 135 kV/cm near the top of the gap.
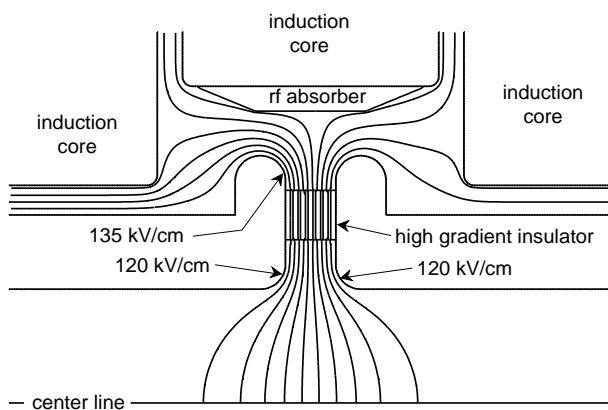

Figure 7. Equipotential lines in vicinity of module gap.

2.4 Mechanical Design Considerations

The insulator is comprised of seven 1 mm layers of polycarbonate alternating with six 0.5 mm layers of conductor. This configuration was also used in the AMOS and Poisson simulations. The insulator fabrication procedure will incorporate additional, larger conductors on either end that are used for mounting the insulator into the gap. These two conductors will be preformed with a 0.5 cm radius of curvature, 90° bend on the inner radius and welded to the beam line at a point of low surface electric field stress to create the vacuum seal. On their outer radius, the conductors have a 180° bend terminating in an electrical slip connection that rides on the magnet housing. This arrangement reduces stress on the insulator due to module housing motion or thermal expansion.

The microwave absorber is segmented ferrite sections epoxied to the inner radius of the center core support mandrel. The AMOS simulations used a TDK PB11b ferrite model.

3 SUMMARY

An induction module has been designed that meets the stringent requirements of the TBNLC relativistic klystron. The demonstrated performance of stacked insulators was a critical factor in achieving a satisfactory design. An important feature of these insulators is their ability to withstand high field stress in the presence of intense electron beams. This allowed for a greatly simplified gap design for the specific application presented and can readily be applied to other induction module designs.

4 ACKNOWLEDGMENTS

5 REFERENCES

[1] Juan M. Elizondo and A.E. Rodriguez, "Novel High Voltage Vacuum Surface Flashover Insulator Technology," Proceedings of the XVth International Symposium on Discharges and Electrical Insulation in Vacuum, Vde-Verlag, Berlin, Germany, pp. 198–202 (1992).
[2] S. Sampayan, et al., "High-Performance Insulator Structures for Accelerator Applications", these proceedings.
[3] S. Sampayan, et al., Proceedings 1995 Particle Accelerator Conference, (IEEE), New York, N.Y., pp. 1269–1271.
[4] M. Burns, et al., Proceedings 1991 Particle Accelerator Conference, (IEEE), New York, N.Y., pp. 2958–2960.
[5] T.L. Houck, et al., these proceedings.
[6] S. Eylon, et al., these proceedings.
[7] T. Houck, et al., *IEEE Trans. Plasma Sci.,* vol. 24, p. 938, 1996.
[8] R.J. Briggs, et al., *Part. Acc.*, **18**, pp.41-62, 1985.
[9] J.-S. Kim, .et al., Proceedings 1993 Particle Accelerator Conference, (IEEE), New York, N.Y., pp. 3288–3290.
[10] Birx, D., Phase II Final Report of Contract DAA H01-89-C-0201, 1991.